Int.J. Electrochem. Sci., 14 **(2019)** 11267 – 11278, doi: 10.20964/2019.12.68

International Journal of ELECTROCHEMICAL SCIENCE
www.electrochemsci.org

Study on the Direct Electrochemical Reduction of Fe_2O_3 in NaCl-$CaCl_2$ Melt

Hui Li[1], Lei Jia[1], Jing-long Liang[1], Hong-yan Yan[1], Zong-ying Cai[1] and Ramana G. Reddy[2]*

[1] Key Laboratory of Ministry of Education for Modern Metallurgy Technology, College of Metallurgy and Energy, North China University of Science and Technology, Tangshan 063210, China
[2] Department of Metallurgical and Materials Engineering, University of Alabama, Tuscaloosa, AL 35487, USA
[*]E-mail: 13373150280@163.com

Received: 1 August 2019/ *Accepted:* 27 September 2019 / *Published:* 29 October 2019

The electrochemical reduction kinetics of Fe_2O_3 in melts were investigated by cyclic voltammetry, square wave voltammetry, open circuit potential and i-t curve analyses at 800°C utilizing a Fe_2O_3 cathode filled in a metal pore molybdenum strip and a graphite rod anode. The composition and morphology of the product obtained by different cell voltage electrolysis were analyzed by XRD and SEM. The reduction mechanism of solid Fe_2O_3 was a three-step electronic process, and two electrons were transferred each time to reduce it to metal iron ($Fe_2O_3 \rightarrow Fe_3O_4 \rightarrow FeO \rightarrow Fe$). Among them, Fe_3O_4 and Fe_xO were produced in the process. In addition, an electrolysis voltage of 1.2~3.0 V was selected for constant potential electrolysis to determine the high current efficiency and low energy consumption. Finally, when an electrolysis voltage of 1.2V was applied, metallized iron with a particle size of 5 μm was obtained, and the current efficiency was 95.3%. The energy consumption was 3.35 kWh/kg. These studies provide a reasonable potential range process parameter for the green preparation of metallic iron by molten salt electrolysis.

Keywords: Fe_2O_3; Electrochemistry; Direct Reduction; Reduction Mechanism

1. INTRODUCTION

Steel is one of the most widely used structural materials to date. In 2018, global crude steel production was 1088.6 billion tons, an increase of 4.6% over that of 2017. At present, steel production technology is mostly based on carbon reduction, in which a large amount of CO_2 is released, contributing to the greenhouse effect. Therefore, it is very urgent to introduce a "greener" steelmaking process to solve climate deterioration [1, 2]. A ULCOS (ultra-low CO_2 steelmaking) project with low CO_2 emissions has been established in Europe [3, 4]; additionally, Boston Metal's molten oxide electrolysis (MOE) production of ferroalloy technology has been carried out for a 20

million dollar round of financing in the first industrial scale deployment aimed at reducing greenhouse gas emissions during iron production.

At present, there are some low-carbon or carbon-free power generation methods that have matured, such as nuclear power, wind power, and hydropower; thus, electric energy will become the most widely used cheap and clean energy source in the future [5-10]. The method of preparing iron metal by using low-cost solid Fe_2O_3 with a short, low energy consuming process, along with being environmentally friendly and controllable, has also attracted attention. S. Licht [9] used electrometallurgy to prepare liquid metal iron directly from oxides. This method required operation at temperatures greater than 1538°C and consumed a large amount of energy. The preparation of metallic iron by chloride, molten carbonate salt systems and alkaline solutions with lower melting points has significant advantages. Wang D.H. [1] reported that Fe_2O_3 was carried out in a K_2CO_3-Na_2CO_3 molten salt to prepare metal iron and oxygen. The reduction step was the chemical formation of $NaFe_2O_3$, then $NaFe_2O_3$ was reduced to $NaFeO_2$ and Fe, and finally $NaFeO_2$ was reduced to metallic iron. Li G.M. [5] obtained iron metal in a pure $CaCl_2$ molten salt system with a constant cell voltage of 1.8~3.2 V for 2~20 h. The reduction step was $Fe_2O_3 \rightarrow FeO \rightarrow Fe$ and Fe_3O_4 was detected in the experiment and considered to be composed of FeO and Fe_2O_3. Gao H.P. [11] studied the filling of Mo pores with Fe_2O_3 as a raw material and obtained a diffusion coefficient of 8.2×10^{-6} $cm^2 \cdot s^{-1}$ in pure $CaCl_2$ molten salt at 1108 K. The activation energy is approximately 67.8 kJ/mol. Fe_3O_4 is not detected at a constant potential, and the reduction step is $Fe_2O_3 \rightarrow FeO \rightarrow Fe$. Zou X.L. [12] studied the preparation of dendritic metal iron by direct electrochemical reduction at a voltage of 1.7 V in an alkaline solution of NaOH at 110°C. The reduction step was $Fe_2O_3 \rightarrow Fe_3O_4 \rightarrow Fe$.

In all studies, Fe_3O_4 is rarely explained in the study of solid Fe_2O_3 reduction. However, according to the Fe-O phase diagram, Fe_3O_4 is a pure substance as a necessary process for the reduction of Fe_2O_3. It is well known that when the temperature is higher than 570°C, the decomposition of Fe_2O_3 is carried out in three steps: $Fe_2O_3 \rightarrow Fe_3O_4 \rightarrow FeO \rightarrow Fe$. This paper uses thermodynamic and kinetic theoretical calculations combined with a variety of electrochemical testing methods, namely, cyclic voltammetry (CV), square wave voltammetry (SWV) and an open circuit potential (OCP-t) method combined with XRD and SEM analysis. The electrochemical reduction of solid Fe_2O_3 in the molten NaCl-$CaCl_2$ system is systematic and detailed. It is a three-step electronic process that transfers two electrons each time and reduces the Fe_2O_3 to iron metal ($Fe_2O_3 \rightarrow Fe_3O_4 \rightarrow FeO \rightarrow Fe$). During the reduction process, Fe_3O_4 and Fe_xO intermediates are produced. The product composition under different constant cell voltages (0.2~3.0 V) was explored, and iron metal was obtained when a smaller electrolysis voltage of 0.6 V was used. A 5-μm mesh iron metal is obtained at a voltage of 1.2 V with a current efficiency of 95.3%, and the energy consumption of producing iron is 3.35 kWh/kg, which is more energy-efficient and environmentally friendly. .

2. EXPERIMENT

2.1 Materials and reagents

The experiments were carried out by using analytically pure NaCl (Sinopharm Chemical Regent Co. Ltd., China, ≥99.95%), $CaCl_2$ (Sinopharm Chemical Regent Co. Ltd., China, ≥99.95%), Fe_2O_3 (Sinopharm Chemical Regent Co. Ltd., China, ≥99.95%), and AgCl (Sinopharm Chemical Regent Co. Ltd., China, ≥99.95%) in a vacuum oven at 260°C for 24 h. The 15×100 mm high-purity graphite rods were polished with 400, 1000, and 2000 mesh sandpaper in sequence, and the graphite surface was repeatedly washed with deionized water and absolute ethanol before being placed in a vacuum oven at 120°C for 48 h. The anode was composed of Φ3 mm stainless steel wire and a graphite rod to form a conductor. The Fe_2O_3 powder was uniformly ground and held under a pressure of 10 MPa for 2 min to obtain a Fe_2O_3 pellet (15 mm in diameter, 2 mm in thickness, 1.0 g in mass, 49% in porosity), which was placed in a tubular resistance furnace and sintered at 800°C for 5 h to obtain sufficient mechanical strength. After cooling, it was wrapped with a 400 mesh and bonded to a 5 mm stainless steel crucible rod to prepare a composite cathode. The corundum crucible containing NaCl-$CaCl_2$ (150 g, molar ratio 42:58) was placed in a tubular resistance furnace raised to 800°C at 5°C/min for 2 h. A stainless-steel wire of 1.0 mm was used as a cathode, and electrolysis was carried out for 2 h at a voltage of 1.8 V. The water remaining in the NaCl-$CaCl_2$ salt and some metal impurities were removed. The experiments were carried out under the protection of high purity Ar (> 99.999%) gas.

2.2 Electrochemical experiment

The CHI660E electrochemical workstation (Shanghai Chenhua, China) was used in the electrochemical test. A three-electrode system was used with a graphite carbon rod (Φ15 mm) as a counter electrode.

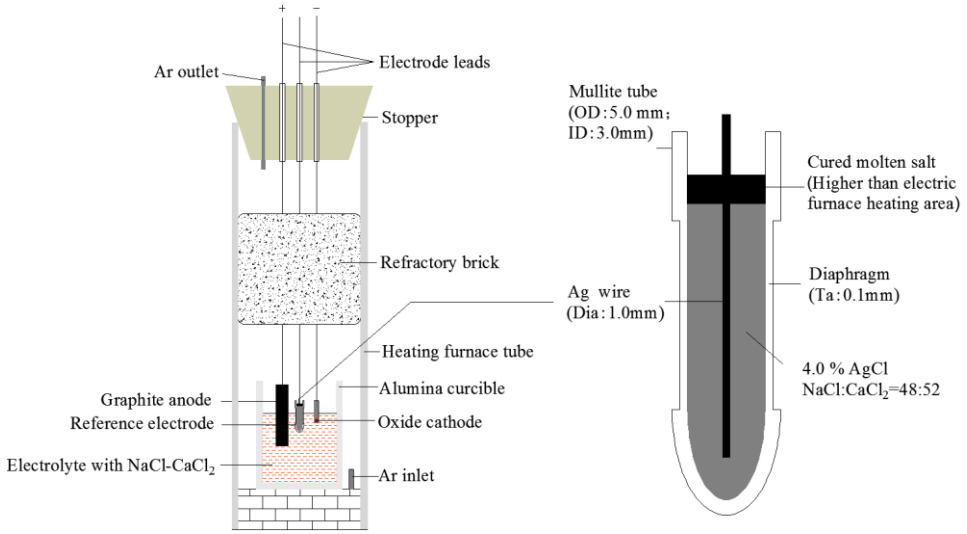

Figure 1. Three-electrode system diagram.

A Ag/Ag^+ reference electrode was prepared by filling an aluminum silicate tube (Φ5 mm) with a molar ratio of NaCl:$CaCl_2$:AgCl=46:50:4 and silver wire (Φ0.5 mm, 99.99%) [13]. A 50 × 2 ×1 mm molybdenum strip with a hole Φ=1 mm at one end was used as the metallic cavity electrode (MCE) [11,14]. The three-electrode system diagram is shown in Fig. 1. All experiments were carried out under high purity argon (> 99.999%).

2.3 Two-electrode constant cell voltage electrolysis

The Fe_2O_3 substrate was electrolyzed for 10 h at different cell voltages (0.2 to 3.0 V) using a GWINSTEK PSM-3004 DC power supply. The cathode was a Fe_2O_3 solid after sintering at 800°C for 5 h, and the anode was a graphite rod. After the end of electrolysis, the sample was slowly cooled with argon gas to 25°C, and the electrolysis product was ultrasonically washed in a beaker containing alcohol for 30 min to remove the chloride salt and then stored under vacuum. Characterization of the sample was analyzed by scanning electron microscopy (SEM, JEM-2800F), energy dispersive spectroscopy (EDX, EDAX Genesis 7000), and X-ray diffraction spectroscopy (XRD, X-ray 6000 with Cu Kα1 radiation λ = 1.5405 Å).

3. RESULTS AND DISCUSSION

3.1 Kinetics considerations

When the molar volume of the metal ($V_m = M_m / \rho_m$, M represents the molar mass, ρ represents the density) and the equivalent molar volume ratio of the corresponding oxide ($V_o = M_o / n \cdot \rho_o$, n represents the number of metal atoms in the oxide formula) are less than 1 ($V_m/V_o<1$), the molten salt will contact the inner oxide, and the oxygen ions can diffuse through the pores of the metal layer to complete the electrodeoxidation reduction [15]. In the case of Fe_2O_3, V_{Fe2O3}=15.237, n=2, V_{Fe3O4}=14.90, n=3, V_{FeO}=12.6, V_{Fe}=7.106, and the iron oxide V_m/V_o of each level is less than 1. Therefore, it is feasible to analyze the molten iron electrodeoxidation method to prepare iron metal. It can be seen from the Fe-O phase diagram that the high-valent oxide is decomposed into low-valent oxides step by step, and finally, iron metal is obtained. Iron exists in a body-centered cubic α-Fe form below 912°C. Fe_2O_3 contains 30% oxygen. The Oxygen occupies the octahedral gap in iron. The combination is firm, and electrolysis deoxidation requires a longer electrolysis time.

3.2 Cyclic voltammetry measurements

First, the reduction mechanism of Fe_2O_3 in NaCl-$CaCl_2$ eutectic melt was studied by CV.

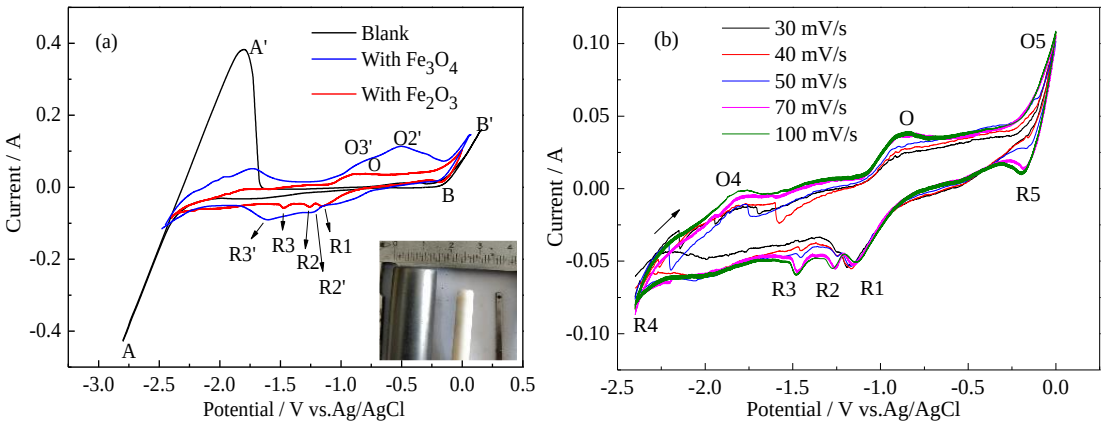

Figure 2. (a) Cyclic voltammetry curve with a scan rate of 70 mV/s and (b) CVs at different scan rates (Scan rates: 30~100 mV/s) in 800°C NaCl-$CaCl_2$ melt with 0.5 mg Fe_2O_3 in MCE. (Insert: Electrode physical map).

Table 1. Gibbs free energies and decomposition voltages of Fe_2O_3 calculated from HSC Chemistry 6.0

Decomposition reaction (T=800°C)	ΔG^{θ} (kJ/mol)	E^{θ}/V (vs. O_2/O^{2-})
$6Fe_2O_3=4Fe_3O_4+O_2(g)$	175.228	-0.45
$2Fe_3O_4=6FeO+O_2(g)$	370.320	-0.96
$2FeO=2Fe+O_2(g)$	299.517	-1.01
$2NaCl=2Na+Cl_2(g)$	575.887	-2.98
$CaCl_2=Ca+Cl_2(g)$	635.34	-3.292
$2CaO=2Ca+O_2(g)$	1045.428	-2.708

Fig. 2(a) is a cyclic voltammetry curve of the molybdenum metal hole electrode (MCE) before and after filling with Fe_2O_3, and a scan rate of 70 mV/s. The red line in Fig. 2(a) is the cyclic voltammetry curve of unfilled Fe_2O_3. Four peaks appear in a scan range of -2.8~0.4 V, where peak A and peak A' are the reduction peak and oxidation peak of Na, respectively. The peak B' corresponds to the formation of chlorine, and the formation of peak B is caused by the change of ion concentration in the nearby molten salt due to the generation of chlorine gas, which increases the rate of reduction of surrounding ions and increases the current [15]. There are no obvious oxidation peaks and reduction peaks in the range of -2.4~-0.4 V; thus, this range can be used as the potential scanning range after filling the MCE with Fe_2O_3. The black and blue curves in the figure are the CVs after filling Fe_2O_3 and Fe_3O_4, respectively. To avoid the influence of the chloride molten salt system, the scanning range is between -2.4~0 V.

According to thermodynamic calculations, the data obtained are shown in Table 1. The thermodynamic analysis shows that the reduction of Fe_2O_3 to Fe_3O_4 is more positive than that of Fe_3O_4 to FeO, meaning it is the more preferred reaction. It is clear in the cyclic voltammogram that the three reduction peaks suggest that Fe_2O_3 is a three-step reduction of metallic iron. Peak R1 should be deoxidized by iron oxide to reduce $Fe_2O_3 \rightarrow Fe_3O_4$, while R2 and R2' are reacted from $Fe_3O_4 \rightarrow FeO$, and the reduction peaks R3 and R3' are the final reduction from FeO to Fe.

Fig. 2(b) is a CV of the scan range with a scan rate of 30~100 mV/s. The oxidation peak O and the reduction peaks R1, R2, and R3 appear under different scan rates. As the scan rate

increases, the oxidation peak O becomes more pronounced because when the faster scan rate is used, the reduction time is shorter; thus, some O^{2-} that is ionized from the Fe_2O_3 matrix does not have enough time to transfer to the anode, but remains at the Fe_2O_3/NaCl-$CaCl_2$ interface, forming a large concentration gradient and increased current. In addition, the remaining O^{2-} participates in the reduction of the iron metal during the subsequent reverse scan, resulting in a strong oxidation peak of O. When a slower scanning speed is applied, oxygen ions are sufficiently transported from the Fe_2O_3/NaCl-$CaCl_2$ interface, and the concentration gradient is reduced, resulting in a decrease in the oxidation peak of O [16]. The reduction peak current R1, peak R2, and peak R3 also decrease. Even at 30 mV/s, the reduction peaks R2 and R3 completely disappear, which can be attributed to more O^{2-} diffused to the anode in the Fe_2O_3 matrix during the long-term reduction process. At the interface of the Fe_2O_3 and NaCl-$CaCl_2$ molten salt, the concentration of oxygen ions decreases, the concentration gradient is small, resulting in a reduced peak current, and the reduction peaks R2 and R3 disappear [2, 11, 14,].

3.3 Square wave voltammetry and open circuit potential measurements

A square wave voltammetry and open circuit potential method was used to study the electrochemical reduction behavior of Fe_2O_3 deoxidation on a Mo electrode in a NaCl-$CaCl_2$ molten salt system. The data obtained are shown in Fig. 3. In the square wave graph of Fig. 3(a), three distinct peaks appear: peak R1 (-1.11 V), peak R2 (-1.43 V), and peak R3 (-1.84 V). There are three platforms in the open circuit potential curve, namely, platform R1 (-1.1 V), platform R2 (-1.5 V), and platform R3 (-1.7 V), as shown in Fig. 3(b). The potentials of the two are similar. The deoxidation reaction of iron oxide on the cathode is a three-step electron reduction process. Thus, $Fe_2O_3 \rightarrow Fe_3O_4 \rightarrow FeO \rightarrow Fe$ is consistent with the conclusion of the cyclic voltammetry curve.

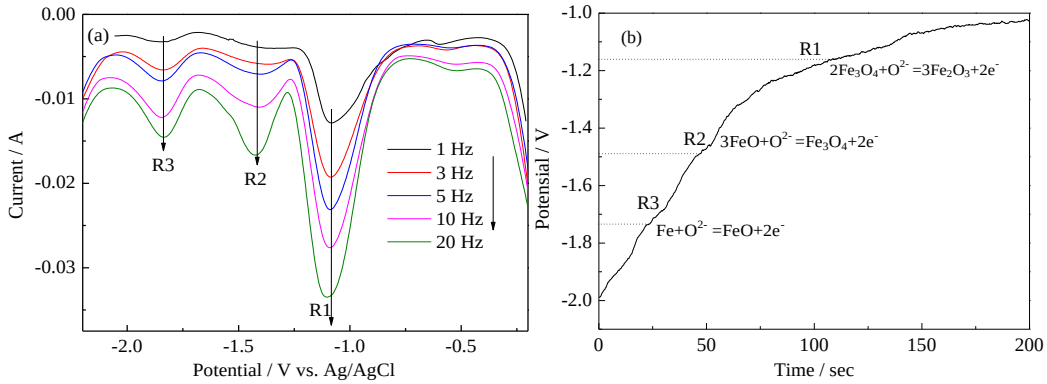

Figure 3. (a) SWV at different frequencies and (b) open circuit potential after 60 seconds of cathodic polarization at 2 V in the NaCl-$CaCl_2$ molten salt at 800°C.

The reduction process of solid Fe_2O_3 determined by square wave voltammetry is shown in Fig. 4(b). Three peaks, R1, R2, and R3, consistent with the results of cyclic voltammetry, can be seen from the figure. The number of electron transfers is calculated by the half width ($W_{1/2}$). [17,18]

$$W_{1/2} = 3.52 \times \frac{RT}{nF} \qquad (1)$$

where R(8.314J·mol^{-1}·K^{-1}) is the molar gas constant, T(K) is the temperature, n is the electron transfer number and F(96485C·mol^{-1}) is Faraday's constant.

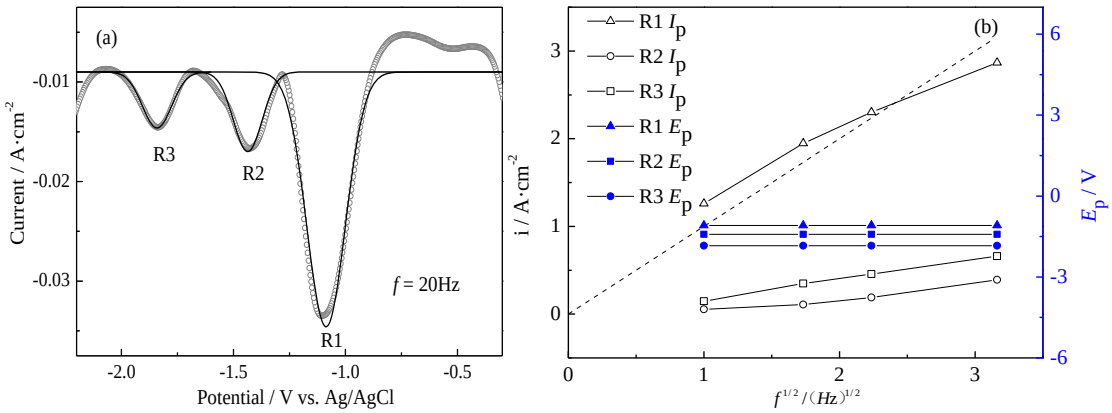

Figure 4. (a) SWV performed in the NaCl-$CaCl_2$ melt and (b) the relationships between peak current density, peak potential and square root of frequency of the R1, R2, and R3 peaks.

The current density of peaks R1, R2, and R3 is linear with the square root of the frequency. The number of electron transitions of R1, R2, and R3 can be calculated by Eq. (1)[15]. The n value was 1.6 for R1, 2.15 for R2, and 2.11 for R3. This indicates that Fe_2O_3 is electrically reduced to metallic iron by a two-electron transfer process, as shown by reactions R1, R2, and R3.

R1: $3Fe_2O_3+2e^-=2Fe_3O_4+O^{2-}$

R2: $Fe_3O_4+2e^-=3FeO+O^{2-}$

R3: $FeO+2e^-=Fe+O^{2-}$

3.4 Two-electrode electrolysis at different cell voltages and product analyses

Fig. 5 is an XRD pattern of an electrolysis product. When a constant potential electrolysis of 0.2 V is applied, an intermediate product of Fe_3O_4 is produced, and Fe_xO begins to appear when electrolysis is applied at 0.3 V. From the Fe-O phase diagram, the formation of this phase is due to the solid solution of the Fe_3O_4 phase into FeO during deoxidation. When a voltage of 0.5 V is applied for 10 h, only Fe_xO is produced, and the Fe_3O_4 phase disappears. When the applied voltage is between 0.6 V and 1.1 V, metallic iron begins to be produced. When an electrolytic voltage greater than 1.2 V is applied, the reduction is completely metallic iron. This process only shows the change law of the oxides of the variable elements. The high-valent oxide will be decomposed into low-valent oxides step by step, and finally, the metal is obtained.

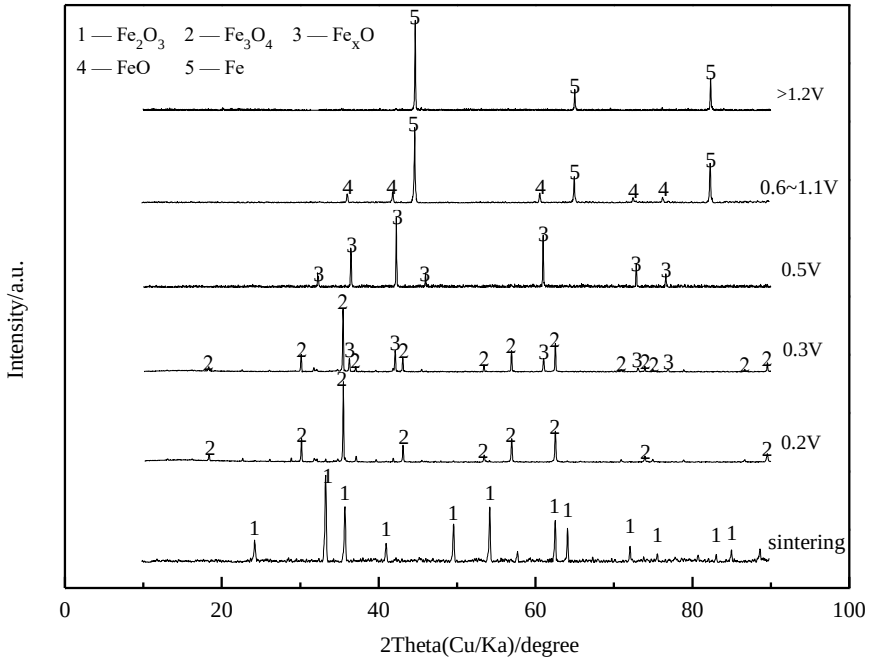

Figure 5. XRD pattern of Fe_2O_3 and electrolysis products obtained by electrolysis at a constant cell voltage in the 800°C NaCl-$CaCl_2$ molten salt (molar ratio: 48:52).

The SEM image of Fig. 6 is an electrolysis sample obtained by sintering at 800°C for 5 h and electrolysis at a potential of 1.2 V, 1.5 V, and 3.0 V for 10 h. Fig. 6(a) shows that the Fe_2O_3 particles grow after sintering at 800°C for 5 h, forming a skeleton structure with a diameter of 200-500 nm, which will facilitate the increase of conductivity and the transfer of O^{2-} from the inside of the particles to the surface of the particles. Fig. 6(b) shows an SEM image of a constant potential electrolysis at a voltage of 1.2 V.

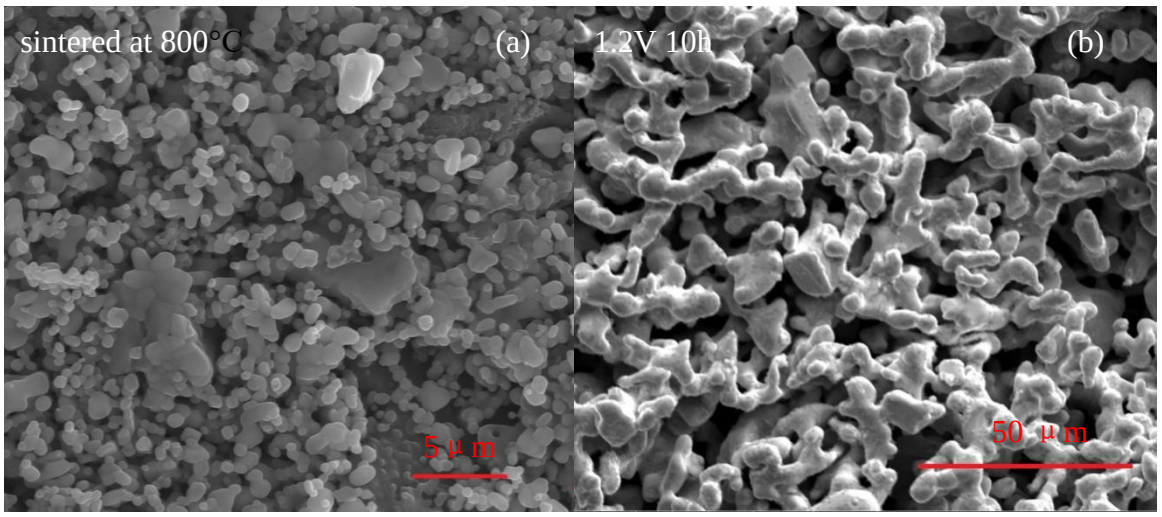

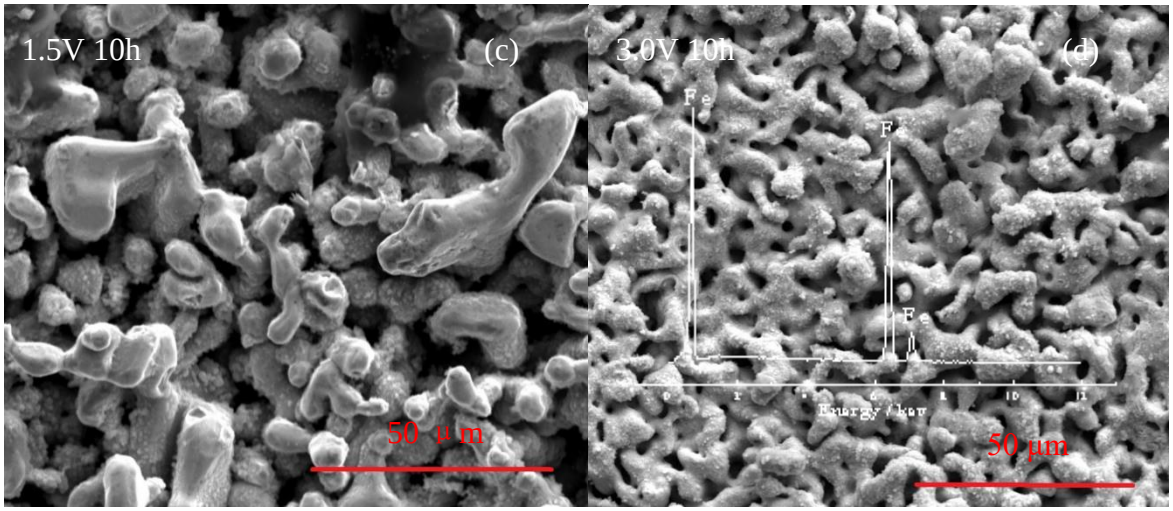

Figure 6. (a) SEM images of sintered Fe_2O_3 pellets (10 MPa, 800°C, 5 h), and (b) after constant cell electrolysis at 1.2 V, (c) 1.5 V and (d) 3.0 V in an 800°C NaCl-$CaCl_2$ eutectic for 10 h. (Insert shows the EDX identification).

The iron particles grow, and the particle size increases to 5 μm. Fig. 6(c) shows the application of a voltage of 1.5 V for constant cell voltage electrolysis, and the iron particle size continues to increase up to approximately 10 μm. Fig. 6(d) is a constant cell voltage electrolysis in which a voltage of 3.0 V is applied, and the iron particles are now interconnected to form a network structure. These results indicate that the morphology of the iron product is controlled by applying different cell voltages. In the electrochemical reduction process, iron oxides are reduced to iron atoms and the iron atoms aggregate to form iron particles. Different voltages can be applied to control the reduction rate of Fe_2O_3, the number of nucleation and the growth rate, which in turn affects the morphology of the reduced product [19].

The data obtained from the recorded time current curve are shown in Fig. 7. In the first stage, the current is large due to the reduction of surface iron. A new Fe/Fe_2O_3/molten salt three-phase reaction boundary forms and extends longitudinally along the surface of the Fe_2O_3 substrate[20,22]. In the second stage, the current decreases rapidly. The reduction reaction of Fe_2O_3 is an exothermic reaction. The Fe metal formed on the surface of the substrate is partially sintered. The metal layer is dense, which hinders the relatively slow mass transfer and the electrons from the inside of the Fe_2O_3 matrix to the molten salt. The conduction and reaction speed is slowed down, the current is reduced, and the appearance of multiple current platforms also indicates that the reduction of Fe_2O_3 is carried out in multiple steps. In the third stage, the current enters the stable phase to reach the background current[19]. In the fourth stage, the current rises only when a voltage higher than 3.0 V is applied, which may be due to the interconnected iron particles produced by reduction. The iron particles produced by the reduction are gradually interconnected, increasing the electron conductivity of the iron layer, and the current is increased [12]; additionally, it may be due to the loss of the graphite anode during the electrolysis process, the deposition of calcium metal, and the formation of $CaCO_3$[23,24]. These side reactions will result in higher energy consumption

and lower current efficiency[5]. The ion transfer model of the electrodeoxidation process of the Fe_2O_3 matrix and the XRD analysis of the molten salt after electrodeoxidation are shown in Fig. 8. The calculation of the efficiency and energy consumption of the Fe_2O_3 electrochemical reduction current under different electrolysis conditions is shown in Table 2 [25].

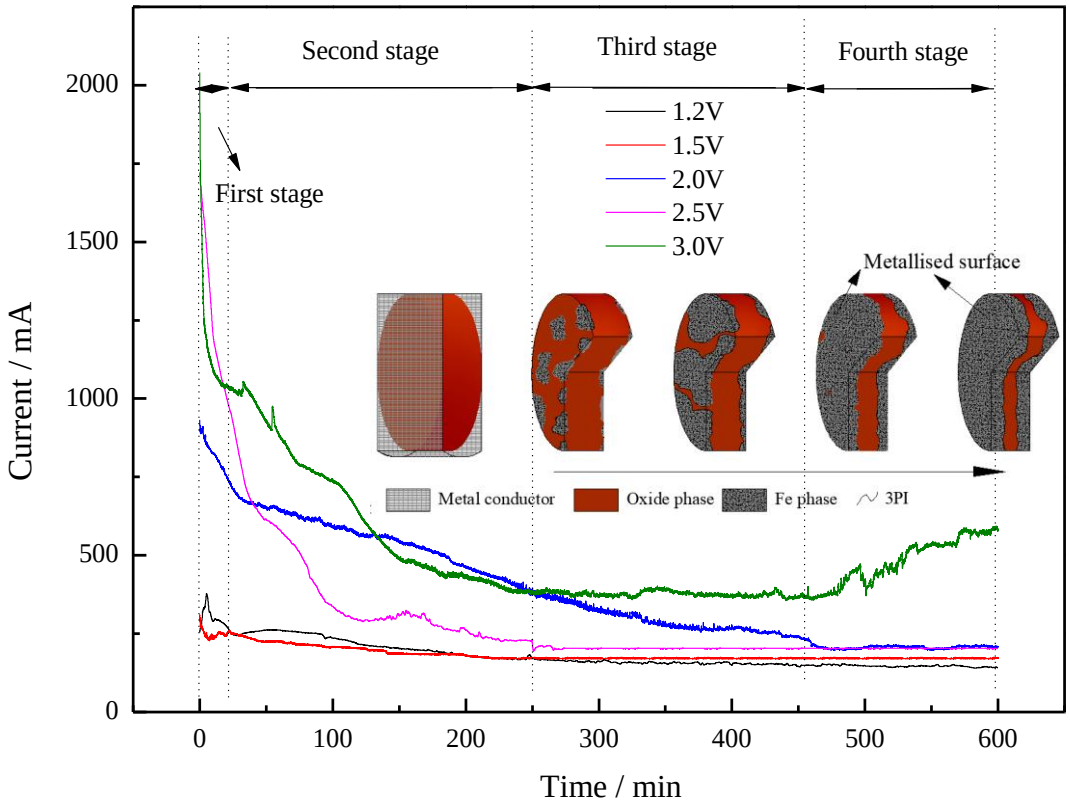

Figure 7. Current time plots of electrolysis for 10 h at different cell voltages in an 800°C NaCl-$CaCl_2$ molten salt system. (Insert shows the propagation of the three-phase Fe/Fe_2O_3/salt and the metallization of the oxide surface)

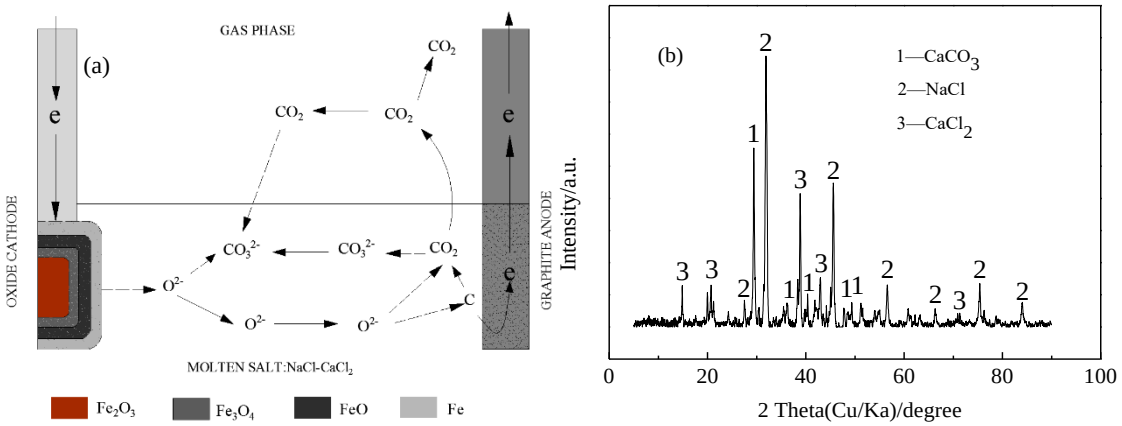

Figure 8. (a) Ion transfer model for the electrodeoxidation process of the Fe_2O_3 matrix and (b) XRD analysis of the molten salt after electro-deoxidation.

Table 2. Calculation of current efficiency and energy consumption of the Fe_2O_3 electrochemical reduction under different electrolysis conditions

Electrolysis conditions	Mass of Fe_2O_3 (g)	Actual consumed electric quantity (mA·h)	Current efficiency (%)	Energy consumption-Fe (kWh/kg)	Actual mass of electrode product-Fe (g)	Theoretical recovery quality -Fe (g)
1.2 V10 h	0.9773	1819	95.3	3.35	0.652	0.68411
1.5 V10 h	0.9592	1848	90.3	4.57	0.606	0.67144
2.0 V10 h	0.9463	3890	83.5	14.07	0.553	0.66241
2.5 V10 h	0.9274	3086	84.6	14.05	0.549	0.64918
3.0 V10 h	0.9704	5243	70.8	32.63	0.482	0.67928

4. CONCLUSIONS

The electrochemical behavior of electrodeoxidation of solid Fe_2O_3 in a NaCl-$CaCl_2$ melt with a molar ratio of 48:52 was investigated by cyclic voltammetry, square wave voltammetry, an open circuit potential method and an i-t curve at 800°C. The composition and morphology of the products obtained by different constant cell voltage electrolysis were analyzed by XRD, SEM and EDX methods. The conclusions obtained are as follows:

1) The reduction of solid Fe_2O_3 in NaCl-$CaCl_2$ molten salt is carried out by a three-step electron transfer that transfers two electrons per step ($Fe_2O_3 \rightarrow Fe_4O_3 \rightarrow FeO \rightarrow Fe$).Finally, metal iron is obtained, and Fe_3O_4 and Fe_xO are produced in the process.

2) The process is a kinetic model of the three-phase reaction boundary line that conforms to the metal/solid oxide/molten salt from the outside to the inside. By controlling the constant cell voltage electrolysis, the morphology of the reduction product can be controlled.

3) Finally, when an electrolysis voltage of 1.2 V is applied, the electrolysis can be completely reduced after 10 h and metallized iron with a particle size of 5 μm is obtained with a current efficiency of 95.3%. The energy consumption is 3.35 kWh/kg. The data obtained can be used as a basis for the industrial preparation of metallic iron and alloys by solid Fe_2O_3 molten salt electrolysis.

FUNDING INFORMATION
The study is financially supported by the National Natural Science Foundation of China (Project No. 51674120，51564016), the Hebei Province Higher Education Science and Technology Research Project (Project No. BJ2017050) and the Graduate Student Innovation Fund of North China University of Science and Technology (Project No. 2019S01).

References

1. D.H. Wang, A.J. Gmitter And D.R. Sadoway, *J. Electrochem. Soc*., 158 (2011) 51.
2. D.Y. Tang, H.Y. Yin, W. Xiao, H. Zhu, H. Mao and D.H. Wang, *J. Electroanal. Chem.*, 689 (2013) 109.
3. A. Allanore, H. Lavelaine, G. Valentin, J.P. BiratAnd F. Lapicque, *J. Electrochem. Soc*., 154

(2007) 187.
4. A. Allanore, H. Lavelaine, G. Valentin, J.P. Birat, P. Delcroix And F. Lapicque. *Electrochim. Acta,* 55 (2010) 4007.
5. G.M. Li, D.H. Wang And Z.Chen, *J. Mater. Sci. Technol.,* 25 (2009) 767.
6. A. Cox, D.J. Fray And J. *Appl. Electrochem.,* 38 (2008) 1401.
7. W. Xiao And D.H. Wang, *Rare Met.,* 35 (2016) 581-590.
8. H.Y. Yin, D.Y. Tang, D.Y., H. Zhu, Y. Zhang And D.H. Wang. *Electrochem Commun*., 13 (2011) 1521.
9. S. Licht, H.J Wu, Z.H Zhang And H. Ayub, *Chem. Commun.,* 47 (2011) 3081.
10. S.L. Wang, G.M. Haarberg And E. Kvalheim, *J. Iron. Steel Res*., 15 (2008) 48.
11. H.P. Gao, X.B. Jin, S.W. Zou, F.Z. Ling, J.J. Peng, Z.Y. Wang And Z. Chen, *Electrochim. Acta*, 107 (2013) 261.
12. X.L. Zou, S.L. Gu, X.G. Lu, X.L. Xie, C.Y. Lu, Z.F. Zhou And W.Z. Ding. *Metall and Mater Trans B.,* 46 (2015) 1262.
13. Y.Q. Wang, R.S. Lin, G.A. Ye, H. He, H.B Tang And Y.H. Jia. *Modern Chemical Industry***,** 35 (2015) 21.
14. L.B Rong, R. He, Z.Y. Wang, J.J. Peng, X.B. Jin And Z.C. George, *Electrochimica. Acta*, 147 (2014) 352.
15. W. Weng, M.Y. Wang, X.Z. Gong, Z. Wang, D. Wang And Z.C. Guo. *Electrochimica. Acta.*, 164 (2017) 551.
16. G. Chen, Z.E. Gordo And D.J. Fray. *Metall. Mater. Trans. B*., 35 (2004) 223.
17. H. Hu, Y. Gao, Y. Lao, Q. Qin, Li, G And G.Z. Chen. *Metall Mater Trans B*., 49 (2018) 2794-2808.
18. Y.J. Hu, X. Wang, J.S. Xiao, J.G. Hou, S.Q. Jiao And H.M. Zhu, *J. Electrochem. Soc*., 160 (2013) 81.
19. D.Y. Tang, H.Y. Yin, X.H. Cheng, W. Xiao And D.H. Wang, *J. Hydrogen. Energy*, 41 (2016)18699.
20. D.S.M. Vishnu, N. Sanil, L. Shakila, G. Panneerselvam, R. Sudha, And K.S. Nagarajan, *Electrochim. Acta*, 100 (2013) 51.
21. D.J.S. Hyslop, A.M. Abdelkader, A. Cox And D.J. Fray, *Acta Mater*., 58 (2010) 3124.
22. W. Xiao, X.B. Jin, Y. Deng, D.H. Wang, X.H. Hu And G.Z. Chen, *Phys. Chem.,* 7 (2006) 1750.
23. W. Weng, L. Tang And W. Xiao, *J. Energy. Chem.,* 28 (2019) 128
24. W. Xiao And D.H. Wang, *Rare Metals.*, 35 (2016) 581-590.
25. M. Shi, S. Li And H. Zhao, *J. Electrochem., Soc.,* 165 (2018) 768-772.